

# Electron-Deficient N-Heteroaromatic Linkers for the Elaboration of Large, Soluble Polycyclic Aromatic Hydrocarbons and Their Use in the Synthesis of Some Very Large Transition Metal Complexes

Yulia Fogel,<sup>†</sup> Marcel Kastler,<sup>†</sup> Zhaohui Wang,<sup>‡</sup> Denis Andrienko,<sup>†</sup>  
Graham J. Bodwell,<sup>†,#</sup> and Klaus Müllen<sup>\*†</sup>

Contribution from the Max Planck Institute for Polymer Research, Ackermannweg 10, D-55128 Mainz, Germany, Beijing National Laboratory for Molecular Sciences, Key Laboratory of Organic Solids, Institute of Chemistry, Chinese Academy of Sciences, Beijing 100080, P. R. China, and Chemistry Department, Memorial University, St. John's, Newfoundland, Canada A1B 3X7

Received April 11, 2007; E-mail: muellen@mpip-mainz.mpg.de

**Abstract:** The selective oxidation of the perimeter of an extended polycyclic aromatic hydrocarbon (PAH), namely a six-fold *tert*-butylated tetrabenzob[*bc,ef,hi,uv*]ovalene, led to the formation of an  $\alpha$ -diketone. The newly installed carbonyl centers allowed this building block to be converted into the largest known heteroatom-containing PAHs (up to 224 atoms in the aromatic core) by way of the quinoxaline ring condensation reaction. The *tert*-butyl substituents caused a distortion of the usually planar aromatic frameworks, which hampered the aggregation tendency of the extended aromatic  $\pi$ -systems and led to extraordinarily high solubilities. All of the systems described here, even the giant phthalocyanine, could thus be purified using standard chromatographic techniques and characterized using typical spectroscopic methods. For the first time, fully resolved <sup>1</sup>H NMR spectra of soluble, diamagnetic, 98- and 104-atom-containing aromatic systems are presented. The computed and experimental UV/vis spectra emphasize the dependence of the characteristic  $\alpha$ -,  $\rho$ -, and  $\beta$ -bands upon the size of the PAHs. It was also possible to obtain the largest known ligand to yet be complexed around a ruthenium center. A quadrupolar solvatochromic effect was observed when two donating PAH moieties were fused to an accepting quinoxaline center, in which case the photoluminescence spanned a range of about 80 nm. Electrochemical properties of the new nanographenes were investigated using cyclic voltammetry, and this showed quasi-reversible reductions.

## Introduction

Polycyclic aromatic hydrocarbons (PAHs) have long been the focus of interdisciplinary research.<sup>1–3</sup> Much of the pioneering work in the direct synthesis and characterization of PAHs was done by Scholl,<sup>4</sup> Clar,<sup>5</sup> and Zander.<sup>5,6</sup> Classical synthetic methods tended to involve relatively vigorous reaction conditions, such as high temperatures and pressures. The trend in recent years is toward the development of much milder methods, with better regioselectivity and higher yields. A representative example of a synthetically easy accessible PAH is hexa-*peri*-

hexabenzocoronene (HBC).<sup>7,8</sup> HBC materials are very interesting due to their physical properties,<sup>9,10</sup> which can be exploited in organic electronic devices, such as field-effect transistors, injection layers, and solar cells.<sup>7,11</sup>

Our strategy for the synthesis of extended PAHs of different sizes and shapes relies on the synthesis of a soluble oligophenylene precursor with a well-defined structure, which is then planarized via cyclodehydrogenation.<sup>12,13</sup> Increasing the surface area of the aromatic core leads to a more pronounced  $\pi$ -stacking propensity, but it also reduces solubility and thus complicates purification, characterization, and processing.<sup>14,15</sup> Improved solubility is normally achieved by introducing long alkyl chains

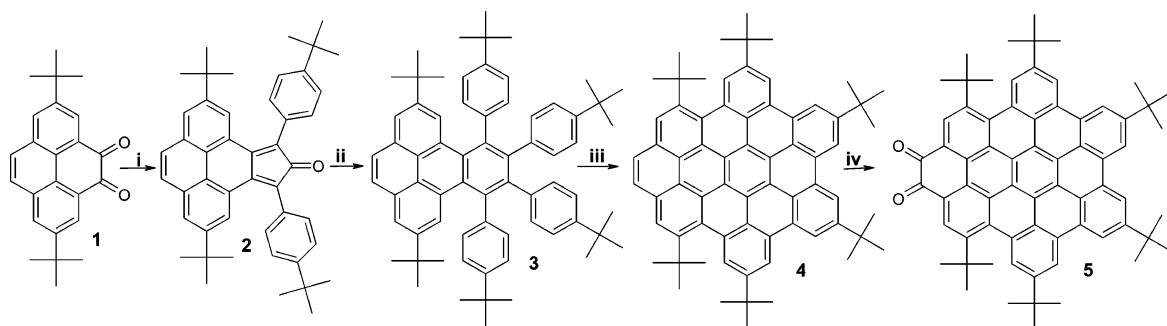
<sup>†</sup> Max Planck Institute for Polymer Research.

<sup>‡</sup> Chinese Academy of Sciences.

<sup>#</sup> Memorial University.

- (1) Armstrong, B.; Hutchinson, E.; Unwin, J.; Fletcher, T. *Environ. Health Perspect.* **2004**, *112*, 970–978.
- (2) Watabe, T.; Ishizuka, T.; Isobe, M.; Ozawa, N. *Science* **1982**, *215*, 403–405.
- (3) Henning, T.; Salama, F. *Science* **1998**, *282*, 2204–2210.
- (4) Scholl, R.; Seer, C.; Weitzenbock, R. *Ber. Dtsch. Chem. Ges.* **1910**, *43*, 2202–2209.
- (5) Clar, E. *Polycyclic Hydrocarbons*; Academic Press: New York, 1964; Vol. 1, p 2.
- (6) Zander, M. *Handbook of Polycyclic Aromatic Hydrocarbons*; Dekker: New York, 1983.

- (7) Kastler, M.; Pisula, W.; Wasserfallen, D.; Pakula, T.; Müllen, K. *J. Am. Chem. Soc.* **2005**, *127*, 4286–4296.
- (8) Pisula, W.; Menon, A.; Stepputat, M.; Lieberwirth, I.; Kolb, U.; Tracz, A.; Siringhaus, H.; Pakula, T.; Müllen, K. *Adv. Mater.* **2005**, *17*, 684–689.
- (9) van de Craats, A. M.; Warman, J. M.; Fechtenkötter, A.; Brand, J. D.; Harbison, M. A.; Müllen, K. *Adv. Mater.* **1999**, *11*, 1469–1472.
- (10) Meijer, E. W.; Schenning, A. P. H. J. *Nature* **2002**, *419*, 353–354.
- (11) Schmidt-Mende, L.; Fechtenkötter, A.; Müllen, K.; Moons, E.; Friend, R. H.; MacKenzie, J. D. *Science* **2001**, *293*, 1119–1122.
- (12) Watson, M. D.; Fechtenkötter, A.; Müllen, K. *Chem. Rev.* **2001**, *101*, 1267–1300.
- (13) Berresheim, A. J.; Müller, M.; Müllen, K. *Chem. Rev.* **1999**, *99*, 1747–1785.

Scheme 1. Synthetic Route to  $\alpha$ -Diketone<sup>a</sup>

<sup>a</sup> Conditions: (i) 1,3-Bis(4-*tert*-butylphenyl)propan-2-one, KOH, EtOH, 80 °C, 15 min, 78%. (ii) Bis(4-*tert*-butylphenyl)acetylene, Ph<sub>2</sub>O, 240 °C, 6 h, 80%. (iii) FeCl<sub>3</sub>, CH<sub>2</sub>Cl<sub>2</sub>, 25 °C, 20 min, 95%. (iv) RuCl<sub>3</sub>/NaIO<sub>4</sub>, CH<sub>2</sub>Cl<sub>2</sub>/CH<sub>3</sub>CN/H<sub>2</sub>O, room temperature, 16 h, 28%.

in the corona of the aromatic system.<sup>16</sup> However, a conceptually different way of enhancing solubility was recently discovered, in which the slight distortion from planarity of a PAH consisting of 72 skeletal carbon atoms led to an enormous increase in the solubility.<sup>15</sup>

In other work in our group, a new protocol was recently established for the synthesis of extended PAHs with high local electron densities in the perimeter, which permitted selective oxidations to the corresponding  $\alpha$ -diketones.<sup>17</sup> Herein, we present a synthetic concept where, by applying the quinoxaline condensation of such  $\alpha$ -diketones, it is possible to grow PAH structures with up to 224 atoms in the core part. The improved solubility of heteroatom-containing PAHs synthesized in this way, by their distortion from planarity by *tert*-butyl groups, allowed nanographenes to be purified and characterized by standard techniques.

## Results and Discussion

**Synthesis and Characterization.** A six-fold *tert*-butylated tetrabenzo[*bc,ef,hi,uv*]ovalene (**4**) was obtained in a stepwise manner as outlined in Scheme 1. The key step for the synthesis of **4** is the cyclodehydrogenation of **3**. Using anhydrous FeCl<sub>3</sub> as both an oxidant and a Lewis acid, **4** was synthesized in nearly quantitative yield.<sup>17</sup> Modification of the previously reported oxidation conditions for the generation of the  $\alpha$ -diketone **5** led to a significant increase in the reaction yield.<sup>17,18</sup> The use of RuCl<sub>3</sub>/NaIO<sub>4</sub> in an aqueous mixture of solvents CH<sub>2</sub>Cl<sub>2</sub>/CH<sub>3</sub>CN, instead of RuO<sub>2</sub>/NaIO<sub>4</sub> in aqueous *N,N*-dimethylformamide, was found to be beneficial in terms of both the yield and the reaction time. Taking all of the difficulties associated with the direct oxidation of the K-region into account (for example, oxidation could proceed in different positions or yield other products), the 28% yield is satisfactory. Compound **5** exhibited good solubility in common organic solvents, presumably due to a distortion of the aromatic core from planarity by bay region *tert*-butyl groups (see Supporting Information).<sup>17</sup> Purification was achieved by column chromatography. The combination of good solubility and the presence of the  $\alpha$ -diketone render compound **5** a promising building block for the construction of larger aromatic and heteroaromatic systems.

**Heteroatom-Containing Nanographenes.** The quinoxaline ring formation between  $\alpha$ -diketones and *o*-phenylenediamines is known to be a high-yielding reaction, which has even been used for the synthesis of polymers.<sup>19–22</sup> To test the condensation conditions for our systems, compound **5** was treated with *o*-phenylenediamine dihydrochloride in boiling acetic acid (Scheme 2). The extended quinoxaline-containing PAH **6** was isolated in 55% yield after 7 h of reaction. Significant amounts of the starting material **5** (up to 20%) were recovered. Three days of reaction furnished 76% of **6** and 5% of **5**. Eventually, the  $\alpha$ -diketone unit **5** is not very reactive. The PAHs **7** and **8** were obtained after the analogous treatment of **5** with 3,3'-diaminobenzidine tetrahydrochloride and 1,2,4,5-benzenetetraamine tetrahydrochloride, respectively.

The large PAHs **6–8** showed good solubilities (up to 20 mg/mL) in common organic solvents such as toluene, THF, and dichloromethane and could thus be purified using standard chromatographic techniques. Unlike all other PAHs of this size, these nanographenes do not have solubilizing long alkyl chains on the corona. The calculated (B3LYP/6-31g\*, vacuum) structure of **8** has significant deviations from planarity, whereas the analogous arene without the *tert*-butyl groups was calculated to have a perfectly planar aromatic framework (Figure 1). Thus, the good solubility arises from either the nonplanarity of the PAH or the presence of the *tert*-butyl groups, or both effects.

Good solubilities allow, contrary to most previously prepared extended PAHs,<sup>23</sup> the recording of structure-rich UV/vis as well as resolved <sup>1</sup>H NMR spectra of the nanographenes **6–8**. Indeed, nanographene **8** is now the largest known PAH system for which a well-resolved <sup>1</sup>H NMR spectrum could be recorded (Figure 2). The sharp aromatic resonances imply a low self-association propensity in solution. Typically, the signals for such systems are broad due to pronounced interactions between the aromatic  $\pi$ -systems.<sup>15</sup>

UV/vis absorption spectra of PAHs **6–8** were recorded in chloroform at a concentration of 10<sup>-5</sup> mol/L (Figure 3). The typical absorption bands for PAHs, designated by Clar<sup>5</sup> as  $\alpha$ ,  $\beta$ , and  $\gamma$ , were observed. In general, the weak  $\alpha$ -band usually appears at the highest wavelength of the three, while the very intense  $\beta$ -band has the lowest wavelength.<sup>24</sup> The  $\beta$ -band usually

(14) Tomovic, Z.; Watson, M. D.; Müllen, K. *Angew. Chem., Int. Ed.* **2004**, *43*, 755–758.

(15) Wasserfallen, D.; Kastler, M.; Pisula, W.; Hofer, W. A.; Fogel, Y.; Wang, Z. H.; Müllen, K. *J. Am. Chem. Soc.* **2006**, *128*, 1334–1339.

(16) Pisula, W.; Kastler, M.; Wasserfallen, D.; Mondeshki, M.; Piris, J.; Schnell, I.; Müllen, K. *Chem. Mater.* **2006**, *18*, 3634–3640.

(17) Wang, Z.; Tomovic, Z.; Kastler, M.; Pretsch, R.; Negri, F.; Enkelmann, V.; Müllen, K. *J. Am. Chem. Soc.* **2004**, *126*, 7794–7795.

(18) Hu, J.; Zhang, D.; Harris, F. W. *J. Org. Chem.* **2005**, *70*, 707–708.

(19) Fox, M. A.; Voynick, T. A. *J. Org. Chem.* **1981**, *46*, 1235–1239.

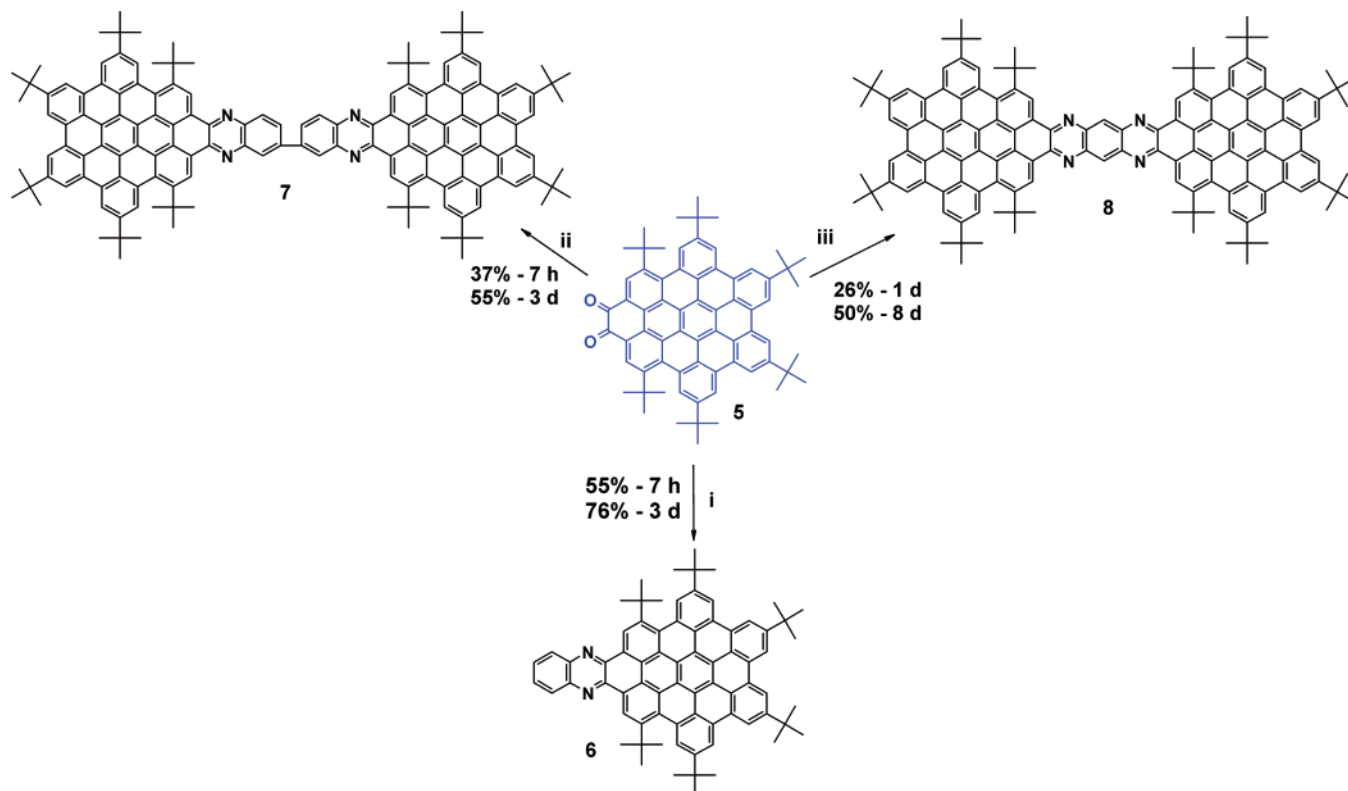
(20) Jenekhe, S. A. *Macromolecules* **1991**, *24*, 1–10.

(21) Sawtschenko, L.; Jobst, K.; Neudeck, A.; Dunsch, L. *Electrochim. Acta* **1996**, *41*, 123–131.

(22) Stille, J. K.; Mainen, E. L. *Macromolecules* **1968**, *1*, 36–42.

(23) Wu, J. S.; Watson, M. D.; Tchebotareva, N.; Wang, Z. H.; Müllen, K. *J. Org. Chem.* **2004**, *69*, 8194–8204.

(24) Fetzer, J. C. *Large (C>=24) Polycyclic Aromatic Hydrocarbons*; John Wiley & Sons: New York, 2000.

**Scheme 2.** Synthesis of Extended Heteroatom-Containing PAHs<sup>a</sup>

<sup>a</sup> Conditions: (i) *o*-Phenylenediamine dihydrochloride, acetic acid, reflux. (ii) 3,3'-Diaminobenzidine tetrahydrochloride, acetic acid, reflux. (iii) 1,2,4,5-Benzenetetraamine tetrahydrochloride, acetic acid, reflux.

**Figure 1.** Optimized geometries of **8** with (left) and without (right) *tert*-butyl groups (B3LYP/6-31g\*, vacuum).

is of intermediate wavelength and intensity and arises from the transition from the highest occupied molecular orbital (HOMO) to the lowest unoccupied molecular orbital (LUMO).<sup>24</sup> PAH **6** has an absorption spectrum similar to that of  $D_{6h}$ -symmetric HBC.<sup>25</sup> However, the usually weak  $\alpha$ -transition is more intense, since the symmetry of **6** ( $C_2$ ) is lower. The absorption spectrum of **7** is very similar to that of **6**, but with a small bathochromic shift (23 nm) of the absorption bands. This is expected since **7** is comprised of two units of **6** connected by a C–C single bond (biaryl linkage). As in most biaryl systems, the electron interaction between the two arenes is relatively small.

In contrast, when two aromatic moieties become fused, as in the nanographene **8**, the absorption spectrum changes dramatically. The longest absorption band shifts bathochromically by about 150 nm. The emission spectra follow a similar trend: the emission maximum of **8** is considerably bathochromically shifted, compared to those of **6** and **7**, which differ only slightly ( $\Delta\lambda = 124$  nm).

To determine the excitation energies, the structures of PAHs **6–8** were first optimized using the Becke three-parameter Lee–Yang–Parr (B3LYP) functional and 6-31G(d,p) basis set. Zerner's intermediate neglect of differential overlap (ZINDO) method was then used to calculate the first 10 excited states.

All calculations were performed using the Gaussian 03 package.<sup>26</sup> The calculations are in good agreement with the experimentally determined peak positions (Table 1), and the error is within the expected range for this type of method.<sup>27</sup>

Both the calculations and the UV/vis data show that an increase in the size of the aromatic system leads to smaller band gaps. With the asymmetric increase of the aromatic system on going from **6** to **8**, the  $\alpha$ - and  $\beta$ -bands exchange their positions. This phenomenon is well-known for the acene series.<sup>5</sup> The energy of  $\beta$ -transitions in the investigated cases does not exhibit a dependence upon the size of the aromatic system.

In order to determine the electron affinity and thus the LUMO levels of the novel PAHs **6–8**, cyclic voltammetry (CV) experiments were performed (Table 2). The PAH **6** exhibits two reversible one-electron reductions, from which a LUMO level of  $-3.53$  eV could be determined. This suggests a reduction of the pyrazine ring, similar to that observed in the known model systems quinoxaline and phenazine.<sup>28,29</sup> Using the optical band gap of 2.56 eV for compound **6**, the HOMO level was determined to be  $-6.09$  eV, which is slightly higher than that

(26) Frisch, M. J.; et al. *Gaussian 03*, Revision B; Gaussian, Inc.: Pittsburgh, PA, 2003.

(27) Parac, M.; Grimme, S. *Chem. Phys.* **2003**, *292*, 11–21.

(28) Alwair, K.; Archer, J. F.; Grimshaw, J. *J. Chem. Soc., Perkin Trans. 2* **1972**, 1663.

(29) Baba, H.; Yamazaki, I. *J. Mol. Spectrosc.* **1972**, *44*, 118–130.

(25) Kastler, M.; Schmidt, J.; Pisula, W.; Sebastiani, D.; Müllen, K. *J. Am. Chem. Soc.* **2006**, *128*, 9526–9534.

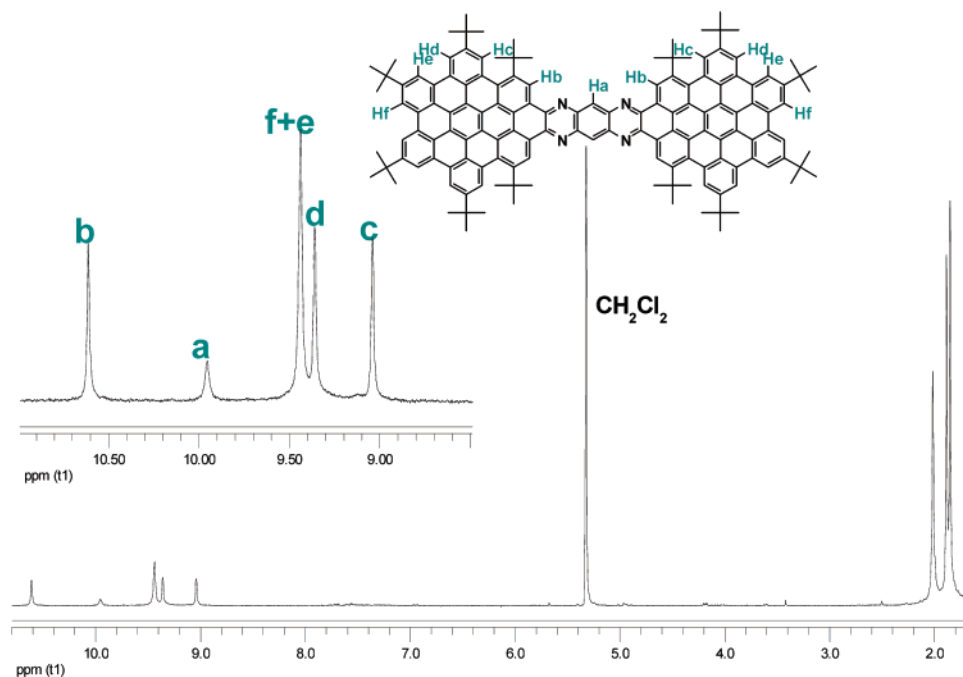


**Figure 2.**  $^1\text{H}$  NMR spectrum of **8** at room temperature (250 MHz, dichloromethane- $d_2$ ).

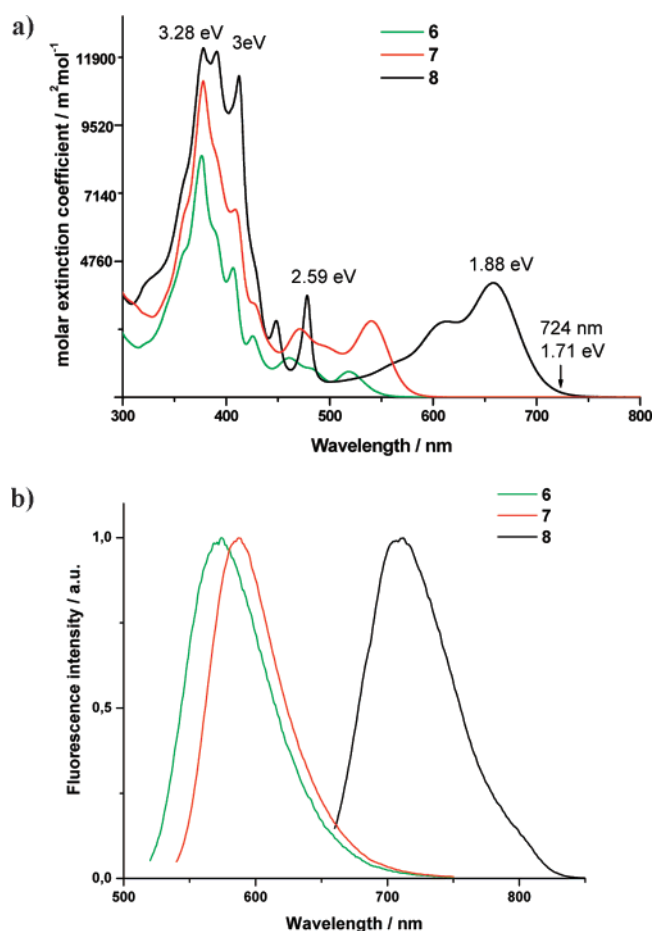


**Figure 3.** (a) Absorption and (b) emission spectra of **6–8** in chloroform at room temperature.

of the model system ( $-6.14$  eV). On going from **6** to the biaryl system **7**, no pronounced changes in the redox potentials were observed. However, both reduction processes of **7** now involve the transfer of two electrons. Although the LUMO energies of

**Table 1.** Comparison between the Calculated Excitation Energies ( $E$ ) and Oscillator Strengths ( $f$ ) and the Experimentally Determined Energies of the PAHs **6–8**

	transition	$E$ (eV)		$f$ (calcd)
		expt	calcd	
<b>6</b>	a	2.39	2.58	0.07
	p	2.56	2.70 <sup>a</sup>	0.03
	b	3.05	2.94	1.19
<b>7</b>	a	2.50	2.57	0.05
	p	2.16	2.52 <sup>b</sup>	0.80
	b	3.03	2.94	0.38
<b>8</b>	a	2.59	2.48	0.11
	p	1.71	2.29	2.19
	b	3.02	3.09	0.0031

<sup>a</sup> Wave function composition:  $-0.34$  (H-1 - L+1),  $0.49$  (H - L).

<sup>b</sup> Wave function composition:  $0.21$  (H-1 - L+1),  $0.38$  (H - L),  $0.13$  (H - L+1).

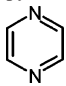
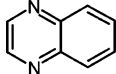
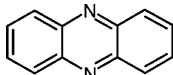
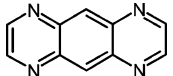
**7** are very similar to those of **6**, the HOMO level was determined to be significantly higher ( $-5.64$  eV). Thus, the increase in the size of the PAH results in an increase of the HOMO level and very little change in the position of the LUMO level. PAH **8** shows two reversible reductions, appearing at more positive potentials than those of the other PAHs and pyrazino[2,3-*g*]-quinoxaline,<sup>30,31</sup> indicating a lower lying LUMO. The extended PAH moieties are in conjugation, and thus the HOMO level is shifted to a higher level ( $-5.41$  eV). Also in this case, as with the pyrazino[2,3-*g*]quinoxaline and **6**, two electrons are transferred in both reduction processes. Worthy of note is that nanographene **8** exhibits an electron affinity similar to that of perylenetetracarboxydiimides, which is one of the most thoroughly studied classes of n-type organic semiconductors.<sup>32</sup> PAH **8** therefore holds promise for use as an n-type organic semiconductor.

(30) Kobayashi, T.; Kobayashi, S. *Eur. J. Org. Chem.* **2002**, 13, 2066–2073.

(31) Ono, K.; Okazaki, Y.; Ohkita, M.; Saito, K.; Yamashita, Y. *Heterocycles* **2004**, 63, 2207.



**Table 2.** Redox Potentials<sup>a</sup>

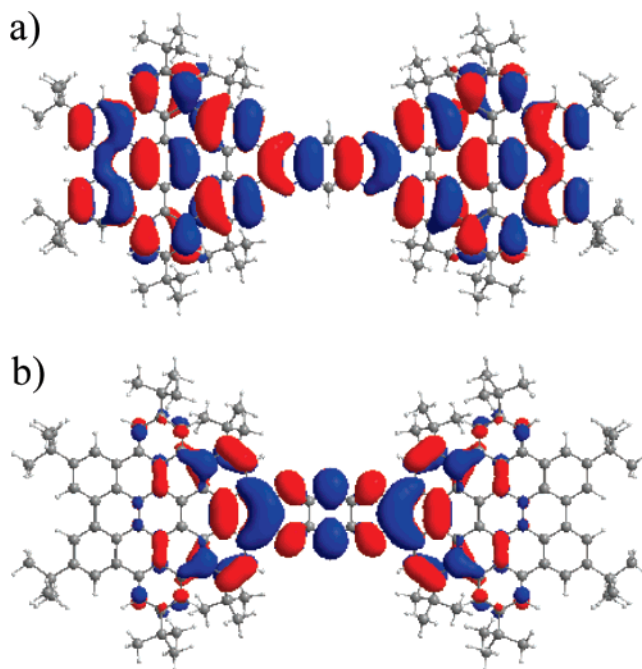
	$E_1^{\text{red}}$ (V)	$E_2^{\text{red}}$ (V)	LUMO (eV)	HOMO– LUMO gap (eV)	HOMO (eV)
pyrazine 	−2.07 (1e)		−2.33	3.75	−6.08
quinoxaline 	−1.62 (1e)	−2.46 (1e)	−2.78	3.92	−6.70
phenazine 	−1.17 (1e)	−1.84 (1e)	−3.23	2.91	−6.14
pyrazino[2,3-g]- quinoxaline 	−0.96 (2e)	−1.54 (2e)	−3.44	3.48	−6.92
<b>6</b>	−0.87 (1e)	−1.38 (1e)	−3.53	2.56	−6.09
<b>7</b>	−0.92 (2e)	−1.35 (2e)	−3.48	2.16	−5.64
<b>8</b>	−0.70 (2e)	−1.10 (2e)	−3.70	1.71	−5.41

<sup>a</sup> Pt electrode vs Ag/AgCl, nBu<sub>4</sub>NClO<sub>4</sub> 0.1 M in CH<sub>3</sub>CN,  $\nu = 100$  mV/s; films were prepared from DCM solution. HOMO values as well as HOMO–LUMO gap were calculated from UV/vis data.<sup>36,37,39</sup>

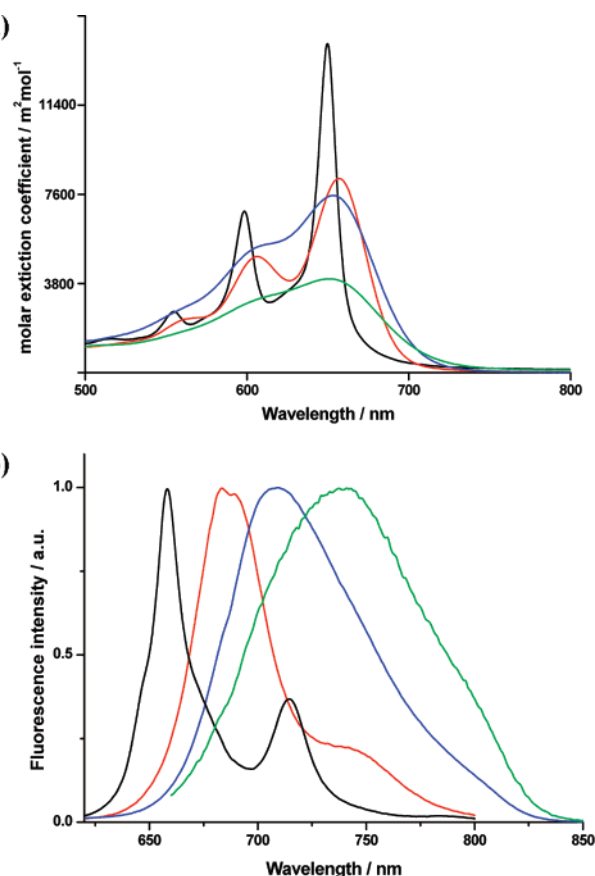
Charge resonance<sup>33,34</sup> is another characteristic feature of organic molecules with electron donor (D) and acceptor (A) groups. Compound **8** is a quadrupolar (D–A–D) molecule. Such systems show a moderately intense absorption band in their UV/vis spectra, which can be assigned to an intramolecular charge-transfer (CT) transition from a localized HOMO into a differently localized LUMO state.<sup>35–40</sup> In the system **8**, the CT band is found at a wavelength of 657 nm (Figure 3). ZINDO calculations show that this band can be assigned to the intramolecular CT transition from the HOMO, delocalized over the HBC framework, to the LUMO, localized on the quinoxaline unit (Figure 4).

Another characteristic feature for small quadrupolar molecules is that the emission is known to shift depending on the solvent polarity.<sup>35–40</sup> UV/vis and emission spectra of compound **8** were recorded in solvents of different polarities, going from cyclohexane to toluene to THF and finally to a mixture of acetonitrile/THF (1/1 by volume). The absorption maximum in the UV/vis spectra (Figure 5a) was found to be insensitive to the solvent polarity (4 nm range). In contrast, the position of the emission maximum undergoes a pronounced bathochromic shift with increasing solvent polarity. The photoluminescence spectrum, recorded in cyclohexane, exhibits a very intense emission at a

- (32) Li, J. L.; Dierschke, F.; Wu, J. S.; Grimdale, A. C.; Müllen, K. *J. Mater. Chem.* **2006**, *16*, 96–100.  
 (33) Kanis, D. R.; Ratner, M. A.; Marks, T. N. *J. Chem. Rev.* **1994**, *94*, 195–242.  
 (34) Terenziani, F.; Painelli, A.; Katan, C.; Charlot, M.; Blanchard-Desce, M. *J. Am. Chem. Soc.* **2006**, *128*, 15742–15755.  
 (35) Chung, S. J.; Rumi, M.; Alain, V.; Barlow, S.; Perry, J. W.; Marder, S. R. *J. Am. Chem. Soc.* **2005**, *127*, 10844–10845.  
 (36) Charlot, M.; Izard, N.; Mongin, O.; Riehl, D.; Blanchard-Desce, M. *Chem. Phys. Lett.* **2006**, *417*, 297–302.  
 (37) Abbotto, A.; Beverina, L.; Bozio, R.; Facchetti, A.; Ferrante, C.; Pagani, G. A.; Pedron, D.; Signorini, R. *Org. Lett.* **2002**, *4*, 1495–1498.  
 (38) Ventelon, L.; Charier, S.; Moreaux, L.; Mertz, J.; Blanchard-Desce, M. *Angew. Chem., Int. Ed.* **2001**, *40*, 2098–2101.  
 (39) Woo, H. Y.; Liu, B.; Kohler, B.; Korystov, D.; Mikhailovsky, A.; Bazan, G. C. *J. Am. Chem. Soc.* **2005**, *127*, 14721–14729.  
 (40) Mongin, O.; Porres, L.; Moreaux, L.; Mertz, J.; Blanchard-Desce, M. *Org. Lett.* **2002**, *4*, 719–722.

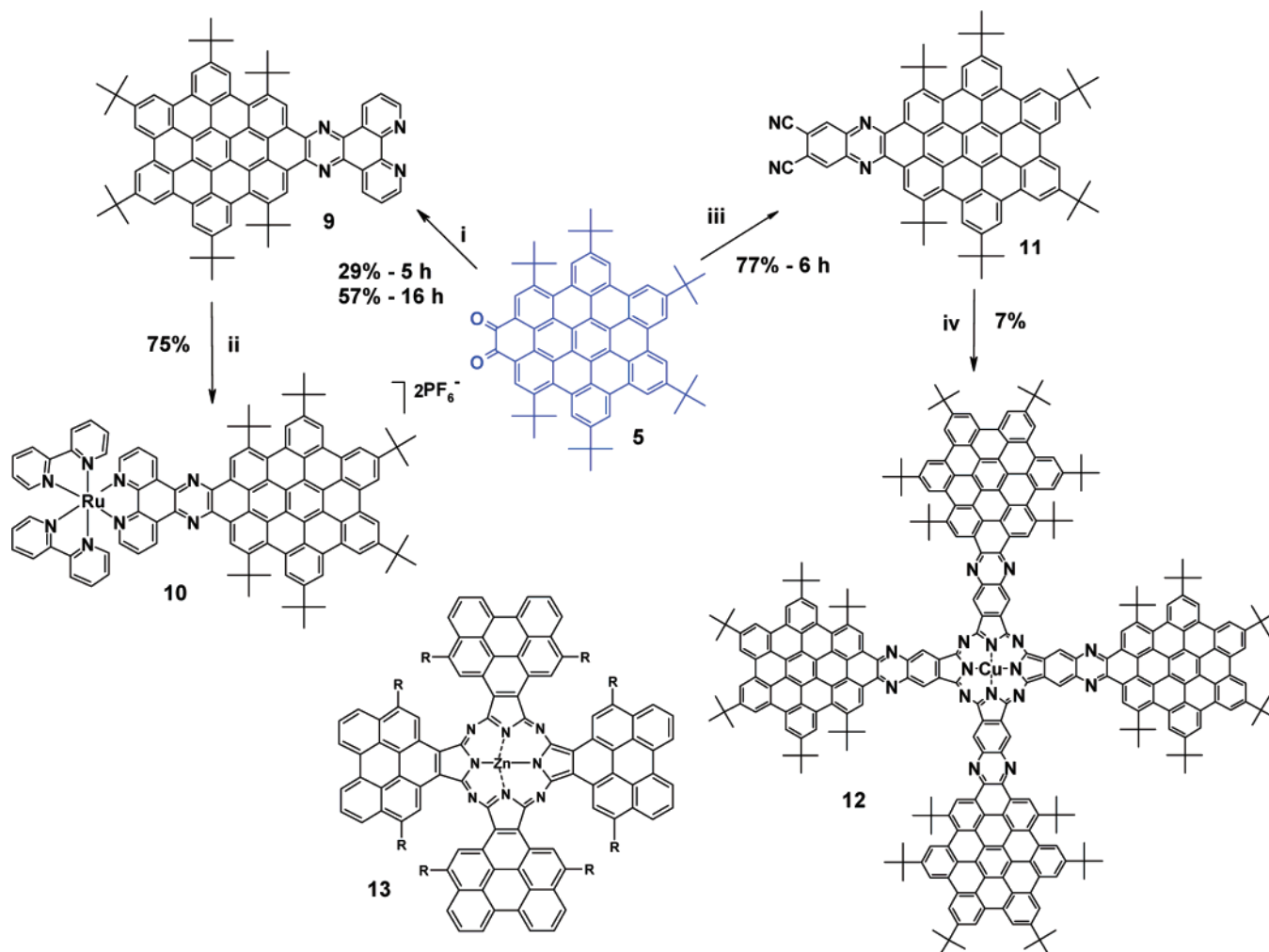


**Figure 4.** Pictorial presentation of (a) the HOMO and (b) the LUMO of **8**, calculated at the B3LYP/6-31g\* level in a vacuum.



**Figure 5.** (a) Absorption and (b) normalized emission spectra of **8** in cyclohexane (black line), toluene (red line), THF (blue line), and a mixture of THF/CH<sub>3</sub>CN = 1/1 (green line).

wavelength of 658 nm (Figure 5b), which shifts to 684 nm in toluene, 709 nm in THF, and 740 nm in a mixture of THF and acetonitrile. This indicates that, even though **8** has no permanent dipole moment (because of its symmetric structure), similar to many families of quadrupolar chromophores, it has a polar

Scheme 3. Synthetic Route to the Extended PAHs<sup>a</sup>

<sup>a</sup> Conditions: (i) 5,6-Diamino-1,10-phenanthroline, pyridine, reflux. (ii) DMF, *cis*-bis(2,2'-bipyridine)ruthenium(II) chloride, reflux, 3 days; precipitation from aqueous  $\text{NH}_4\text{PF}_6$ , 75%. (iii) Acetic acid, 1,2-diamino-4,5-dicyanobenzene, reflux, 6 h. (iv) Urea,  $\text{CuCl}_2$ , quinoline, 220 °C, 16 h.

excited state.<sup>36,37,39</sup> Hence, the tetraazaanthracene bridge in the D–A–D system **8** can function as a  $\pi$ -electron-accepting unit only in the excited state. In this context, **8** is now the largest known PAH system exhibiting fluorescence solvatochromism.

**Metal-Containing Nanographenes.** The quinoxaline condensation reaction using the building block **5** could also be used in the synthesis of very large heterocycles capable of complexation to the metal center. Thus, the condensation reaction of **5** with 5,6-diamino-1,10-phenanthroline<sup>41</sup> gave the heteroarene **9** with 60 atoms in its aromatic framework (Scheme 3). To test whether the phenanthroline-containing PAH **9** is a suitable ligand for metal complexation, it was reacted with *cis*-bis(2,2'-bipyridine)ruthenium(II) chloride to afford the diamagnetic complex **10** (Scheme 3). The formation of **10** was confirmed by <sup>1</sup>H NMR, UV/vis, and MALDI MS.

The reaction of compound **5** with 1,2-diamino-4,5-dicyanobenzene in the quinoxaline condensation afforded the intended dinitrile precursor **11**, which was subsequently reacted with urea in the presence of  $\text{CuCl}_2$  to deliver the giant and largest known phthalocyanine derivative **12** (224 atoms in the aromatic skeleton).<sup>42,43</sup> No product was found in the absence of urea.

Variation of the temperature, concentration, and reaction time, as well as the use of microwave irradiation, did not lead to an improvement of the yield. The low yield of 7% is, in fact, in the same range as those obtained for other “large” phthalocyanines, e.g., one containing 104 skeletal atoms **13** (4%).<sup>44</sup> Most of the unreacted starting material could be recovered.

The UV/vis absorption spectrum of **12** was recorded in chloroform and exhibits the two characteristic bands for phthalocyanines (B- and Q-bands at 379 and 869 nm, respectively), along with bands originating from the PAH **6** moieties (Figure 6).<sup>43</sup> The weak absorption band at about 780 nm is a vibrational overtone of the Q-band.<sup>43</sup> The Q-band, which corresponds to a  $\pi$ – $\pi^*$  transition from the HOMO to the LUMO, is red-shifted by about 190 nm from that of commercially available copper tetra-*tert*-butylphthalocyanine (CuPc). The extended phthalocyanine **13** exhibits a Q-band around 797 nm in its UV/vis spectrum.<sup>44</sup> It is well known that the intensity of the Q-band is very sensitive to substitution and aggregation.<sup>43,45,46</sup> For **12**, the Q-band is less intense than that of CuPc,

(41) Bodige, S.; MacDonnell, F. M. *Tetrahedron Lett.* **1997**, *38*, 8159–8160.

(42) Tomoda, H.; Saito, S.; Shiraishi, S. *Chem. Lett.* **1983**, *3*, 313–316.

(43) Mckeown, N. B. *Phthalocyanine Materials*; University Press: Cambridge, 1998.

(44) Cammidge, A. N.; Gopee, H. *Chem. Eur. J.* **2006**, *12*, 8609–8613.

(45) Cook, M. J.; Dunn, A. J.; Daniel, M. F.; Hart, R. C. O.; Richardson, R. M.; Roser, S. J. *Thin Solid Films* **1988**, *159*, 395–404.

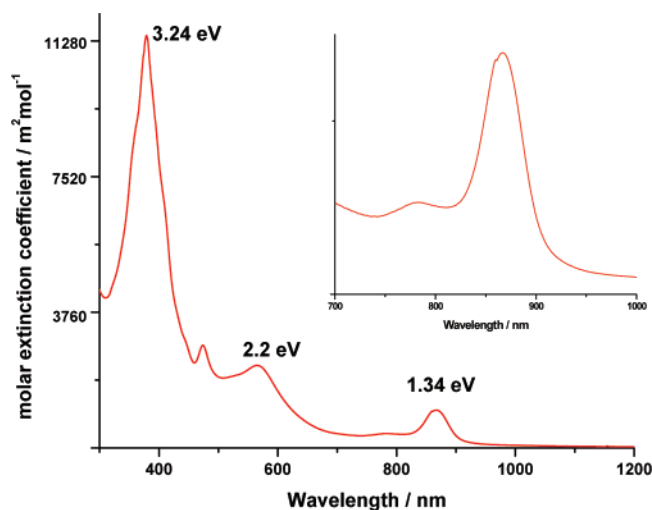


Figure 6. Absorption spectrum of **12**.

which might be due to the distortion from planarity of the aromatic units and the presence of acceptor moieties around the Pc center.<sup>47,48</sup> The other typical absorption band, the B-band or Soret band,<sup>43</sup> was observed at 379 nm. The B-band is assigned to a  $\pi-\pi^*$  transition of the aromatic units fused to the Pc macrocycle. Because of the extended PAH systems in **12**, this band is about 2 times more intense than those of CuPc. Using CV and the optical band gap, the energies of the HOMO ( $-3.59$  eV) and LUMO ( $-4.93$  eV) of **12** were obtained. The energy gap of **12** is much smaller than those of small Pc derivatives.<sup>49,50</sup>

Not unexpectedly for a paramagnetic compound,<sup>51,52</sup> the  $^1\text{H}$  NMR spectrum of copper phthalocyanine **12** exhibits one very broad signal in the aromatic region. However, the signals for the *tert*-butyl protons, which are farther removed from the copper center, could be resolved.

## Conclusions

The selective oxidation of the perimeter of a six-fold *tert*-butylated tetrabenzob[*bc,ef,hi,uw*]ovalene, **4**, led to the formation of an  $\alpha$ -diketone, **5**. This versatile building block took part in quinoxaline reactions to afford several giant heteroatom-containing PAHs of unprecedented size. The distortion from planarity of the aromatic frameworks of **5** by the bulky *tert*-butyl groups brought extraordinarily high solubilities, presumably through the suppression of aggregation of the aromatic  $\pi$ -systems. Therefore, purification and characterization of all the presented PAHs were achieved using standard methods. The good solubility (up to 20 mg/mL) should allow such huge molecules (up to 224 aromatic atoms in the core) to be easily

processed, which is one of the critical requirements for their implementation in organic electronic devices.

Well-resolved  $^1\text{H}$  NMR spectra were recorded for all diamagnetic nanographenes (**6**, **7**, and **8**). The sharp resonances in the aromatic region implied low self-association propensities in solution. The experimental and computed UV/vis spectra were in good agreement and revealed that the positions of the  $\alpha$ - and  $\beta$ -bands depend strongly on the overall size of the aromatic system. According to CV, the introduction of quinoxaline or tetraazaanthracene bridges into the large aromatic moiety significantly reduced the LUMO level, thus rendering them strongly electron-accepting systems.

The novel nanographene **8**, with 98 atoms in the aromatic core, is so far the largest known PAH with a well-resolved  $^1\text{H}$  NMR spectrum and exhibits strong fluorescence solvatochromism. The emission of **8** shifts with the polarity of the solvent, suggesting that this system can function as a  $\pi$ -electron-accepting unit only in the excited state.

The largest known ligand to be complexed to a metal center has also been synthesized. Ligand **9**, which is composed of 60 skeletal atoms (56 carbon and 4 nitrogen), was used to furnish a ruthenium complex, **10**. Using this approach, it should now be possible to construct a range of large metal complexes by varying the metal as well as the number and nature of the giant ligands.

The copper phthalocyanine **12** is the largest known phthalocyanine derivative. It has an absorption maximum at 865 nm (Q-band) and excellent chemical stability (stable up to ca. 450 °C). This makes it an attractive system for use in long-term archival storage devices, such as write-once, read-many-times disks.<sup>53</sup> Metallophthalocyanines have been demonstrated to possess remarkable semiconducting properties with n-type properties.<sup>54</sup> The small HOMO–LUMO gap makes **12** a potential candidate for applications in n-type organic field effect transistors.<sup>55</sup>

**Acknowledgment.** This work was financially supported by the Deutsche Forschungsgemeinschaft (SFB 625) and the Max Planck Society through the ENERCHEM and NAIMO (NMP4-CT-2004-500355) programs. M.K. thanks the “Fonds der Chemischen Industrie” for financial support. We thank Dr. Martin Baumgarten and Dr. Frédéric Laquai for helpful discussions.

**Supporting Information Available:** Experimental section,  $^1\text{H}$  NMR spectra, MALDI-TOF MS spectra, single-crystal structure, CV data, UV/vis and fluorescence spectra, and complete ref 26. This material is available free of charge via the Internet at <http://pubs.acs.org>.

(46) Cook, M. J.; Dunn, A. J.; Howe, S. D.; Thomson, A. J.; Harrison, K. J. *J. Chem. Soc., Perkin Trans. 1* **1988**, 2453–2458.

(47) Kudrevich, S. V.; vanLier, J. E. *Coord. Chem. Rev.* **1996**, *156*, 163–182.

(48) Kobayashi, N.; Nakajima, S.; Osa, T. *Inorg. Chim. Acta* **1993**, *210*, 131–133.

(49) Cox, G. A.; Knight, P. C. *J. Phys. C: Solid State Phys.* **1974**, *7*, 146–156.

(50) Usov, N. N.; Bendersk, V. *Phys. Status Solidi* **1970**, *37*, 535–537.

(51) Assour, J. M.; Harrison, S. E. *Phys. Rev. A-Gen. Phys.* **1964**, *136*, 1368–1373.

(52) Boguslavskii, E. G.; Prokhorova, S. A.; Nadolinnyi, V. A. *J. Struct. Chem.* **2005**, *46*, 1014–1022.

JA072521T

(53) Emmelius, M.; Pawlowski, G.; Vollmann, H. W. *Angew. Chem., Int. Ed. Engl.* **1989**, *28*, 1445–1471.

(54) Bao, Z. A.; Lovinger, A. J.; Brown, J. J. *Am. Chem. Soc.* **1998**, *120*, 207–208.

(55) Yoon, M. H.; Facchetti, A.; Stern, C. E.; Marks, T. J. *Am. Chem. Soc.* **2006**, *128*, 5792–5801.